Proceedings of the ASME 2023 18th International Manufacturing Science and Engineering Conference
MSEC2023
June 12 ~ 16, 2023, New Brunswick, New Jersey, USA.

MSEC2023-103862

A FRINGE PATTERN ANALYSIS TECHNIQUE FOR PHOTOMASK LINE-EDGE-ROUGHNESS CHARACTERIZATION

Zhikun Wang[1], Kuan Lu[1], ChaBum Lee[1,*]
[1] Texas A&M University, Mike Walker 66' Department of Mechanical Engineering, College Station, TX, 77843, USA

ABSTRACT

Line-edge roughness (LER) characterization is vital in the semiconductor industry. This paper presents an EKEI (enhanced knife edge interferometry)-based method for photomask LER characterization. The changes in fringe pattern caused by edge roughness were derived and analyzed by cross-correlation index. A negative relationship between the cross-correlation and the LER value was observed. The result is validated by both simulation and experiment, indicating that the proposed method can detect both roughness changes and residual pollution on photomask edge.

Keywords: Semiconductor, Photomask, Line-edge-roughness, Edge diffraction, Metrology, Lithography

INTRODUCTION

With the demand for rapidly growing semiconductor industries, lithography-related system is getting increasing attention [1]. During the lithography process, even tiny defect on photomask can greatly compromise the quality of final products. Therefore, the photomask inspection technology, as a potential method to deal with this problem, has became a research hotspot in this area [2]. In photomask inspection, the most critical parameters to be measured include dimension, defect, and LER (line edge roughness) [3-4]. Currently, most used photomask inspection method includes SEM, TEM [5-14] and AFM [15-18]. However, these methods are very expensive and time consuming. Therefore, a high-speed and low-cost inspection method is in high demand. In this study, an EKEI (enhanced knife edge interferometry)-based photomask LER characterization method, which is an improvement of previous developed KEI-based system, is proposed [19-23]. By building a geometrical-based optic model, the LER's influences towards detected fringe patterns can be analyzed. Thus, both edge defects and LER anomaly on photomask can be detected. The performance of this method was verified by both numeral simulation and experiments.

LER EVALUTION PRINCIPLE

The LER measurement principle is based on Fresnel number-based geometry optic model. Figure 1 shows the schematic for the EKEI-based KEI characterization system. The setup is similar to author's previous work [21].

This Fresnel zone-based fringe pattern can be directly estimated using Eq.1 [19]:

$$F = \frac{\alpha^2}{\lambda \times Z_{eff}} \tag{1}$$

where α is the radius of the beam at the photomask plane, λ is the light wavelength, Z_{eff} is the effective distance of the optical system.

In Eq.1, the odd terms of the Fresnel zone provide positive contribution for the recorded intensity while the even term provides negative contribution.

Eq.1 can be converted to [19]:

[*] Corresponding Author: mbgjun@purdue.edu

© 2023 by ASME

$$F = \frac{NA^2 \times Z_{src}}{\lambda} \qquad (2)$$

where NA is the numerical aperture from the objective lens and Z_{src} is the distance from the photomask to the objective lens focal point.

In this paper, the LER is introduced into simulation model. The LER can be defined as 3 times the standard deviation of the edge profile, which is controlled by 2 parameters: duty ratio (D/P) and the intensity (I) shown in Fig.1. Thus, the definition of LER can be re-written as:

$$LER = 3 \times I\sqrt{\frac{D}{P} \times (1 - \frac{D}{P})}. \qquad (3)$$

The Fresnel zone will be blocked by the LER affected edges; thus, the fringe pattern changes with different blocking area. Therefore, LER can be measured by fringe pattern changes.

NUMERICAL SIMULATION

The simulated datasets consist of 10 groups of fringe pattern, among which, nine sets were generated by edges with different LER while the remaining one generated by smooth edge is considered as reference.

As shown in Fig.1(a), the magnitude of fringe pattern decreases when LER increases.

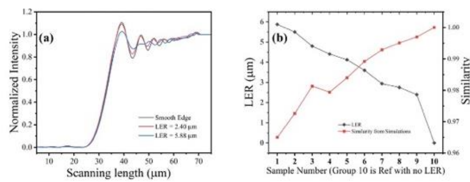

Figure 1. (a) Simulated fringe pattern with different LER conditions, (b) similarity for different LER condition-generated fringe pattern based on cross-correlation method.

The changes in simulated fringe pattern can be further evaluated by a cross-correlation-based method [20], as shown in Fig. 1(b). It is clearly indicated that there is a strong negative correlation between the LER value and the similarity value.

EXPERIMENTS

The system prototype, shown in Fig.2, consists of a well-collimated monochromatic laser diode, a dimension-fixed thin aperture, an ideal objective lens with a certain numerical aperture (NA), a XY-motorized stage, and a PD-assisted op-amp.

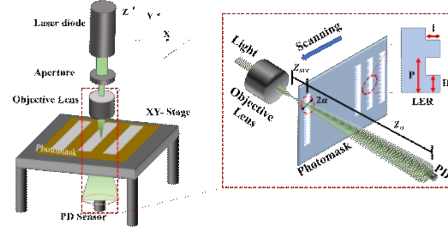

Figure 2. Measurement method: Enhanced knife-edge interferometry

A well-collimated green laser light (λ 532 nm) passes through a ϕ1.0 mm aperture, then further re-shaped by an objective lens (NA = 0.4). Once the light passes through the photomask, it shines on the PD sensor.

The photomask is fixed on a XY-motorized linear stage, its line patterns' fringe pattern are recorded when the stage moves. The scanning speed is 1mm/s with a 25mm moving resolution.

Photo of real experiment setup is shown in Fig.3.

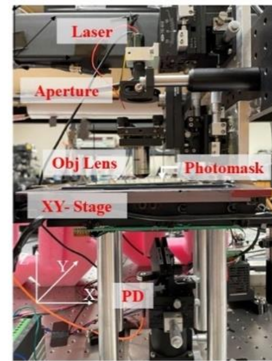

Figure 3. Experiment setup

As discussed in previous part, the cross-correlation index between experiment groups and reference group were calculated to evaluate LER changes. In the design, LER varies from 2.40 μm to 5.88 μm. For verification purpose, the LER value of each line pattern was also measured by optical microscope, as shown in Fig.4.

 © 2023 by ASME

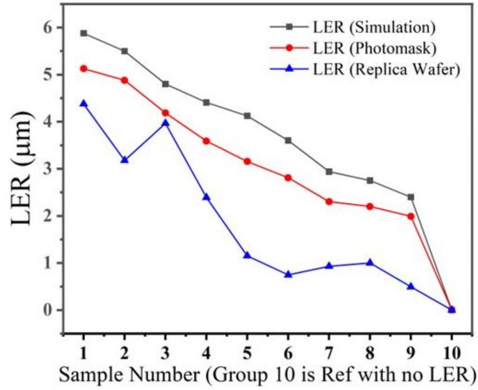

Figure 4. LER values calculated from design, photomask, and printed wafer patterns.

Difference exists between LER values in designed and manufactured samples, which could be caused by the resolution limitation of microscope.

Fig.5 shows how the designed LER line pattern is transferred to real photomask product.

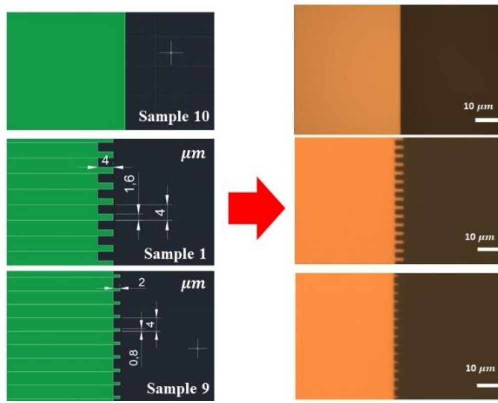

Figure 5. Photomask LER design and images of the fabricated patterns: (a) photomask LER design (left), (b) pictures of real photomask with designed LER

RESULTS

Fringe pattern results of different line edges are shown in Fig.6.

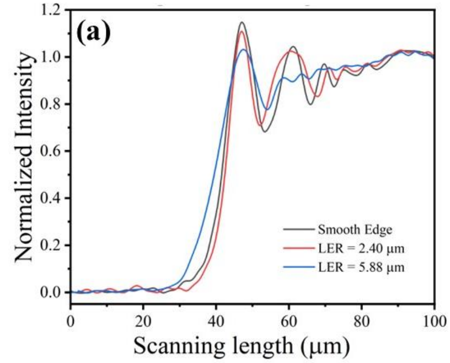

Figure 6. Fringe patterns of photomask cases.

As the LER increases, the intensity for the first order fringe decreases and the high-order fringe is attenuated.

Cross-correlation results are further calculated, as showed in Fig.7.

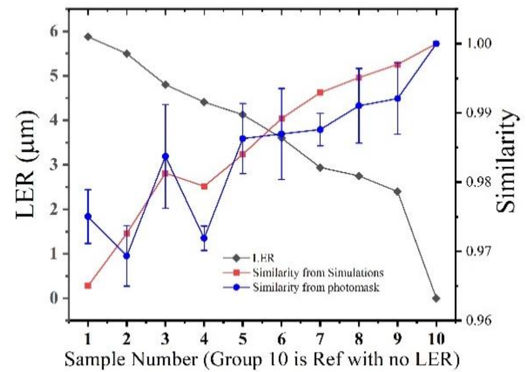

Figure 7. LER characterization: result by cross-correlation method

The similarity decreases while the LER value increasing on the line pattern. When the LER value changes from 2.40 μm to 5.88 μm, the similarity decreases by 0.0183.

Overall, the experiment result agrees with the relationship obtained from simulation. However, slight difference exists between simulation results and experiment data, which could be caused by two factors: alignment error and slightly anisotropic property of glass.

To further evaluate the performance of proposed method, fringe patterns of residual polluted the edge were also measured as shown in Fig.8. The fringe pattern of polluted edge was attenuated at the beginning, then increased gradually. This is

 © 2023 by ASME

because the residual can partially cover the edge but cannot block the light completely. This result indicates that the proposed system might be applied for in-process lithography monitor.

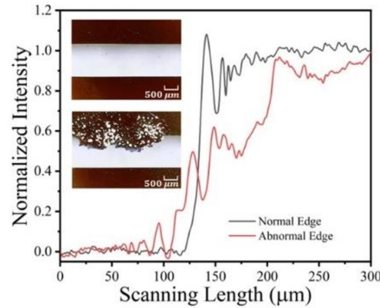

Figure 8. Photomask defect inspection: (a) particles on the photomask and (b) interferometric fringe pattern

Conclusion and future work

This paper proposed an EKEI-based photomask inspection system for LER and defect characterization. A Fresnel number-based geometrical optic modal was built, and a cross-correlation-based method was used for LER evaluation. Through numerical simulation, fringe patterns under various LER conditions were computed and analyzed, strong negative correlation between the cross-correlation index and LER values were observed on the line patterns. Experiment from manufactured photomasks show good agreement with the simulation results. In addition, the methods also show the potential to detect the residual pollution on the edge. For the future work, 1-D wavelet transform method could be employed as a more promising fringe pattern analyze method, which can provide much more profound information of edge characteristic, as shown in Fig.8.

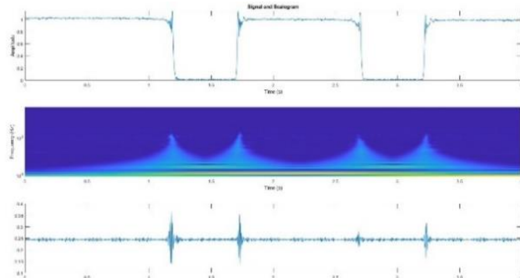

Figure 8. Results from 1-D wavelet transform method

REFERENCE

1. Global Photomask Market – industry trends and forecast to 2029. Photomask Market Size, Share, Growth, & Forecast Analysis By 2029. (n.d.). Retrieved October 5, 2022, from https://www.databridgemarketresearch.com/reports/global-photomask-market
2. Shubham, K., & Gupta, A. (2021). Integrated Circuit Fabrication. CRC Press.
3. Obert Wood, EUV lithography: new metrology challegens, AIP Conference Proceeding 931, 375 (2007).
4. Banqiu and Ajay Kumar, "Extreme ultraviolet lithography: A review", Journal of Vacuum Science & Technology B: Microelectronics and Nanometer Structures Processing, Measurement, and Phenomena 25, 1743-1761 (2007) https://doi.org/10.1116/1.2794048
5. Yoshizawa, M., & Moriya, S. (2002). Study of the acid-diffusion effect on line edge roughness using the edge roughness evaluation method. Journal of Vacuum Science & Technology B: Microelectronics and Nanometer Structures Processing, Measurement, and Phenomena, 20(4), 1342-1347.
6. Winey, M., Meehl, J. B., O'Toole, E. T., & Giddings Jr, T. H. (2014). Conventional transmission electron microscopy. Molecular biology of the cell, 25(3), 319-323.
7. Schorb, M., Haberbosch, I., Hagen, W. J., Schwab, Y., & Mastronarde, D. N. (2019). Software tools for automated transmission electron microscopy. Nature methods, 16(6), 471-477.
8. De Graef, M. (2003). Introduction to conventional transmission electron microscopy. Cambridge university press.
9. Zuo, J. M., & Spence, J. C. (2017). Advanced transmission electron microscopy. New York: Springer Science+ Business Media.
10. Fultz, B., & Howe, J. M. (2012). Transmission electron microscopy and diffractometry of materials. Springer Science & Business Media.
11. Leamy, H. J. (1982). Charge collection scanning electron microscopy. Journal of Applied Physics, 53(6), R51-R80.
12. Vernon-Parry, K. D. (2000). Scanning electron microscopy: an introduction. III-Vs Review, 13(4), 40-44.
13. Zhou, W., Apkarian, R., Wang, Z. L., & Joy, D. (2006). Fundamentals of scanning

 © 2023 by ASME

electron microscopy (SEM). In Scanning microscopy for nanotechnology (pp. 1-40). Springer, New York, NY.

14. Scheinfein, M. R., Unguris, J., Kelley, M. H., Pierce, D. T., & Celotta, R. J. (1990). Scanning electron microscopy with polarization analysis (SEMPA). Review of scientific instruments, 61(10), 2501-2527.
15. Giessibl, F. J. (2003). Advances in atomic force microscopy. Reviews of modern physics, 75(3), 949.
16. Garcıa, R., & Perez, R. (2002). Dynamic atomic force microscopy methods. Surface science reports, 47(6-8), 197-301.
17. Rugar, D., & Hansma, P. (1990). Atomic force microscopy. Physics today, 43(10), 23-30.
18. Meyer, E. R. N. S. T. (1992). Atomic force microscopy. Progress in surface science, 41(1), 3-49.
19. Zhikun Wang, Pengfei Lin, and ChaBum Lee, Preliminary Study of Photomask Pattern Inspection by Beam-Shaped Knife-Edge Interferometry, Precision Engineering, 77, 104-109 (2022).
20. Zhikun Wang and ChaBum Lee, Knife-edge interferogram analysis for corrosive wear propagation at sharp edges, Applied Optics, Vol. 60, Iss. 5, pp. 1373-1379 (2021).
21. Zhikun Wang, Heebum Chun and ChaBum Lee, Enhancement of knife-edge interferometry for edge topography characterization, Review of Scientific Instruments, Vol. 92, 125101 (2021).
22. Seongkyul Jeon, Christopher K. Stepanick, Abolfazl A. Zolfaghari, ChaBum Lee, Knife-edge interferometry for cutting tool wear monitoring, Precision Engineering, Vol. 50, pp. 354-360 (2017).
23. Seongkyul Jeon, Abolfazl Zolfaghari, ChaBum Lee, Dicing wheel wear monitoring technique utilizing edge diffraction effect, Measurement, 121, pp. 139-143 (2018).

 © 2023 by ASME